The basics of probabilistic internal stability analysis and design of reinforced soil walls explained

Richard J. Bathurst
GeoEngineering Centre at Queen's-RMC, Canada

ABSTRACT: This paper explains the basics of probabilistic analysis and design for the internal stability limit states of tensile rupture and pullout in mechanically stabilized earth (MSE) walls. The concepts are general and can be applied to any soil-structure interaction problem which can be expressed by a simple linear limit state performance function. The general approach considers uncertainty in the choice of nominal values and links probability of failure to the underlying accuracy of the load and resistance models that appear in each limit state equation using bias statistics. A useful closed-form solution is presented to calculate margins of safety in terms of reliability index. The formulation is easily implemented in a spreadsheet to facilitate sensitivity analysis during design and thus is an alternative approach to Monte Carlo simulation.

Keywords: probabilistic analysis, MSE walls, internal limit states, tensile rupture, pullout

1 INTRODUCTION

Geosynthetic reinforced soil walls are an accepted category of mechanically stabilized earth (MSE) technologies and their presence is ubiquitous on the geotechnical civil engineering landscape. The analysis and design tools for these systems are most often deterministic in nature and can be traced to adaptations of classical soil mechanics earth pressure theory and limit equilibrium methods.

The internal stability design for MSE walls in the UK is based on a partial factor approach in which factors are applied to soil and reinforcement material properties and to load contributions in different combinations to ensure safe designs. Geotechnical foundation design codes in North America adopt a load and resistance factor design (LRFD) approach which has been used by structural engineers for decades in Canada and the USA. In this approach, load terms are multiplied by load factors (magnitude of one or more) and the resistance side is multiplied by a single resistance factor (with a magnitude of one or less). The intent of a properly calibrated limit state design equation expressed in a LRFD framework is to ensure that a target maximum probability of failure will not be exceeded. However, the load and resistance factors that appear in LRFD codes have been selected largely by fitting to factors of safety used in allowable (working) stress design (ASD) past practice. Whether a designer uses a partial factor approach as in the UK or a LRFD approach as in North America, the margin of safety expressed probabilistically is unknown. This leads to the conundrum of a limit state being satisfactory when viewed from a factor of safety point of view but unsatisfactory from a probability of failure perspective. This point is demonstrated for the case of the rupture and pullout limit states for the geosynthetic reinforcement layers in the MSE wall in Figure 1. The nominal tensile load Q_n can be calculated using one of a number load models found in the literature and design codes. Similarly, the nominal resistance R_n can be calculated for tensile rupture and pullout limit states using equations found in design guidelines. In conventional allowable stress design the ratio of nominal resistance to nominal load defines the factor of safety; the resistance term is adjusted so that the factor of safety satisfies a minimum acceptable value. However, both nominal resistance and nominal load sides have uncertainty as visualized by the idealized frequency distributions in Figure 2. Notionally, the area of the overlap of the lower tail of the resistance distribution on the right with the upper tail of the load distribution on the left indicates a non-zero probability of

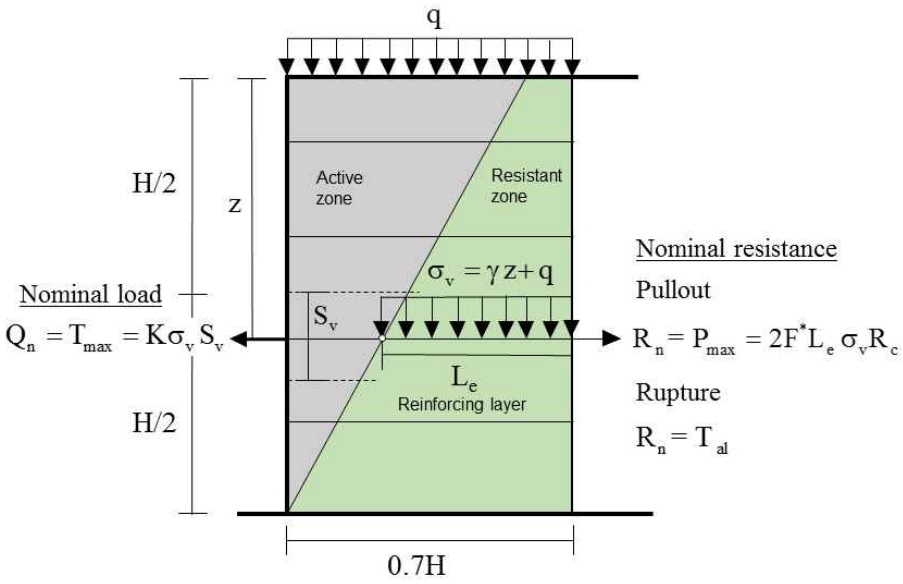

Figure 1. Nominal load and resistance equations for reinforcement rupture and pullout limit states for internal stability of geosynthetic reinforced MSE walls

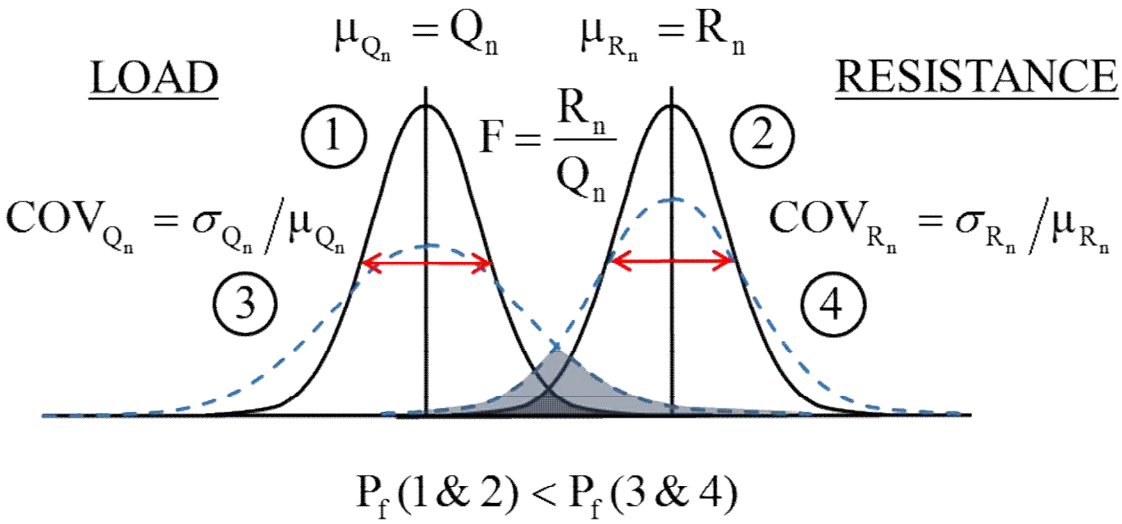

Figure 2. Factor of safety and probability of failure concepts

failure. Clearly, two different combinations of load and resistance distributions can have different probabilities of failure (P_f) while the factor of safety remains the same. The distributions for nominal resistance and load values can be characterized by mean and coefficient of variation (COV) where the latter is simply the standard deviation divided by the mean. These distributions may have different forms but lognormal distributions are the most common for the quantities that are the focus of this paper.

An alternative preferred parameter to quantify margins of safety in geotechnical engineering is reliability index β. The relationship between probability of failure and reliability index is $P_f = 1 - \Phi(\beta)$ where Φ is the standard normal cumulative distribution function (CDF) (NORM.DIST in Excel).

2 FORMULATION OF LIMIT STATE EQUATIONS

If all uncertainty in the true magnitude of load and resistance terms for the limit states introduced above was solely due to the estimation of the soil friction angle (ϕ) and soil unit weight (γ), then the probability of failure of each limit state can be computed using the following equation and Monte Carlo simulation:

$$g = \frac{R_n}{Q_n} - 1 \tag{1}$$

Specifically, random values of ϕ and γ are simulated from probability distributions for these parameters for a total of N times, and each pair of values are used to compute values of R_n and Q_n. Unlike naturally deposited soils, the backfill soil in a MSE wall is an engineered material and therefore the variability in soil unit weight and friction angle are low. For Monte Carlo simulation, COV values of 0.10 and 0.05 for ϕ and γ are reasonable. For large N values, the number of times $g < 0$ divided by N trials (*realizations*) is the probability of failure.

However, the true probability of failure is strongly influenced by the accuracy of the load and resistance models that appear in the formulation of a limit state equation. The expectation that any design equation for Q_n and R_n in geotechnical foundation engineering design will give the actual load or resistance is not reasonable. Furthermore, we expect that different models will have different accuracy when predicted values are compared to measured values. The ratio of measured load or resistance to the corresponding predicted load or resistance is called *method bias* (or *bias* for brevity) and is denoted by λ in this paper. The nominal load and resistance terms in Equation 1 can be transformed to give a performance function that is expressed in terms of true (i.e. measured) values of load (Q_m) and resistance (R_m) terms as follows:

$$g = \frac{\lambda_R R_n}{\lambda_Q Q_n} - 1 = \frac{R_m}{Q_m} - 1 \tag{2}$$

To compute the *true* probability of failure, the same Monte Carlo simulation technique described above is used with the additional steps of also sampling resistance and load bias values from random distributions of λ_R and λ_Q during each realization.

3 LIMIT STATE BIAS STATISTICS AND INTERPRETATION

For the rupture (tensile strength) limit state, the value of λ_R is simply the ratio of estimated tensile strength at end of design life divided by the nominal estimated value. In North American practice the nominal value is the long-term allowable strength T_{al} computed as:

$$T_{al} = \frac{T_{ult}}{RF} \tag{3}$$

Here, T_{ult} is the reference ultimate strength of the reinforcement and RF is a reduction factor that accounts for the loss of tensile strength over the design life of the reinforcement due to creep, installation damage and possible chemical/biological processes. Bias values for tensile strength have been computed by comparing available strength at end of design life (e.g. 75 years) to nominal values using results of product-specific long-term creep rupture testing and installation damage testing. Bathurst and Miyata (2015) developed bias statistics for the combined effect of installation damage and creep on geogrid reinforcement tensile strength at the end of design life for different geogrid classification types. The COV of tensile rupture bias values ranged from 0.04 to 0.14. A value of $COV_{\lambda R} = 0.10$ was judged to be a reasonable typical value. The mean of tensile rupture bias for the same materials was taken as $\lambda_R = 1.10$ (Bathurst et al. 2011). This value follows from North American practice to conservatively report the ultimate tensile strength as the minimum average roll value (MARV) which is computed as the average ultimate tensile strength of a roll that is two standard deviations below the average ultimate tensile strength from multiple rolls. The value of $\lambda_R = 1.10$ means that the true long-term tensile strength of a reinforcement geosynthetic is 10% higher, *on average*, than the certified product value reported for T_{ult} and used in Equation 3.

Bias statistics for the pullout limit state can be gathered from conventional laboratory pullout box testing. In this case, each measured maximum pullout load is compared to the predicted value using a particular model and the same vertical stress used in the test; the bias value is computed as the measured value divided by the predicted value. Bias values computed in this manner can be expected to vary

between different models due to: 1) differences in the ability of the underlying deterministic pullout model (of which there are many) to capture the mechanics of soil-reinforcement interaction during pullout; 2) uncertainty due to variation in pullout box testing protocols; 3) quantity and quality of data, and; 4) consistency in interpretation of data gathered from multiple sources (the typical case) (Allen et al. 2005). As just one example, bias statistics for the same soil and reinforcement type acquired from a laboratory pullout box text may be different from the bias statistics for the same materials and vertical confining stress for tests performed in-situ (Miyata and Bathurst 2012).

Bias values for two different pullout models are plotted as cumulative distribution function (CDF) plots in Figure 3. A total of n = 318 test results were taken from Huang and Bathurst (2009). These plots are created in the following steps: 1) bias values are sorted in rank order from 1 to n by magnitude (lowest bias value first); 2) each value is then assigned a cumulative probability from p = 1/(n+1) to 1; 3) the standard normal variable z is computed as $z = \Phi^{-1}(p)$ where Φ^{-1} is the inverse standard normal distribution function (NORM.S.INV in Excel), and; 4) plot z versus bias. If bias values are normally distributed the data will appear as a straight line on this plot with linear axes. If the bias values are lognormally distributed the data will present as a straight line on a log-linear plot which is the case here for Figure 3. In this figure, the data have also been plotted with cumulative probability as the vertical axis which may be more familiar to readers. For plots of this type (and using generic bias notation λ), the mean of Ln values of λ, denoted as $\mu_{LN\lambda}$, will intersect the horizontal axis at z = 0 and the slope of the line will be the inverse of the standard deviation ($1/\sigma_{LN\lambda}$) of the ln(λ) distribution. The following transformations can be used for $\sigma_{LN\lambda}$ and $\mu_{LN\lambda}$:

$$\sigma_{LN\lambda} = \sqrt{LN(1 + COV_{\lambda}^2)} \tag{4a}$$

$$\mu_{LN\lambda} = LN(\mu_{\lambda}) - \frac{1}{2}\,\sigma_{LN\lambda}^2 \tag{4b}$$

Figure 3 shows pullout bias values using two different pullout models. The pullout model proposed by Huang and Bathurst (2009) is judged to be better than the current AASHTO (2017) model with respect to accuracy because the mean of bias values ($\mu_{\lambda R}$) is closer to one and the spread in bias values expressed by $COV_{\lambda R}$ is much less.

Figure 4 shows the results of bias analysis for the load side for the two limit states introduced in this paper. Load model 1 is the current AASHTO (2017) Simplified Method and load model 2 is the Simplified Stiffness Method (Allen and Bathurst 2015, 2018). The former is a combined soil strength- and reinforcement type-based method to compute maximum tensile reinforcement loads (T_{max} in Figure 1) under operational conditions, while the latter is a reinforcement stiffness-based approach. The load bias values plot as roughly straight lines over most of the data range in Figure 4 confirming, at least visually, that the bias values may be reasonably assumed to be lognormally distributed. There is a discrepancy between the measured data and the fitted approximations at the lower tails, but this is not a practical concern because it is the upper tail that has the most influence on probability of failure as illustrated notionally in Figure 2.

The bias statistics for the two load models demonstrate that the AASHTO (2017) Simplified Method is very conservative because the measured loads are only 40% of predicted loads *on average*. Furthermore, there is large uncertainty in the accuracy of the model which is quantified by the COV of load bias values (i.e. $COV_{\lambda Q}$= 95%). In contrast, the Simplified Stiffness Method is much more accurate on average with only 5% overestimation of maximum tensile loads and less spread in accuracy of predictions quantified by $COV_{\lambda Q}$ = 36%. The reason for the better agreement for the Simplified Stiffness Method is that it accounts for the influence of reinforcement stiffness on magnitude of maximum load in a reinforcement layer (T_{max}) and was empirically calibrated against a large database of measured T_{max} values to give a mean bias value close to one and a minimum COV of load bias values (Allen and Bathurst 2015, 2018).

So far in this paper, possible correlations between nominal values and between bias values and predicted values have not been addressed. These correlations (*dependencies*) are possible depending on the limit state and the models that appear in the limit state design equations. For example, consider Figure 5 which shows pullout bias values plotted against predicted (nominal) (P_{max}) pullout values. The bias values are the same data discussed with Figure 3. Log axes have been used in Figure 5 to spread the data points out for better visual clarity, but this choice of axes does not prejudice the quantitative interpretation described next. The data show that for the poorer pullout model (PM1) the accuracy of the model changes

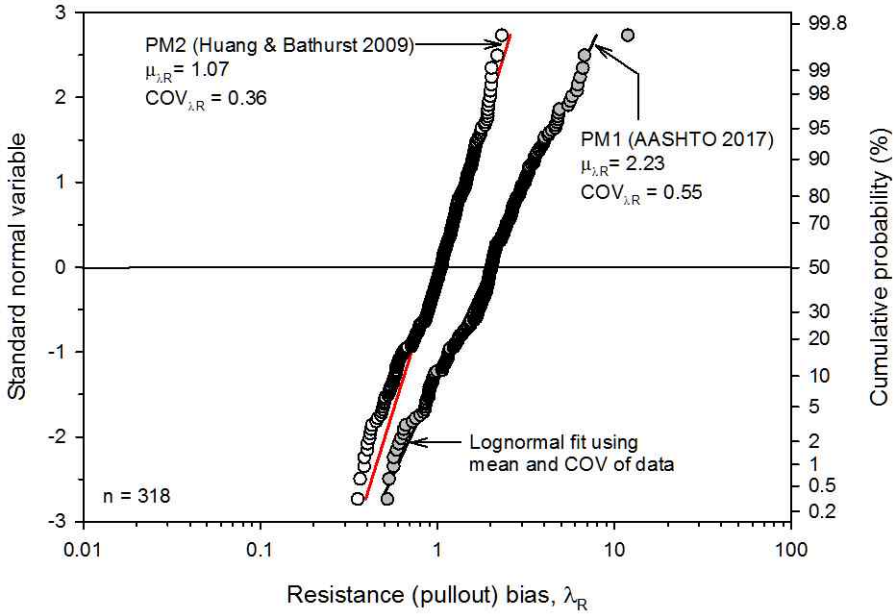

Figure 3. Cumulative distribution function (CDF) plots for pullout bias using two different pullout models

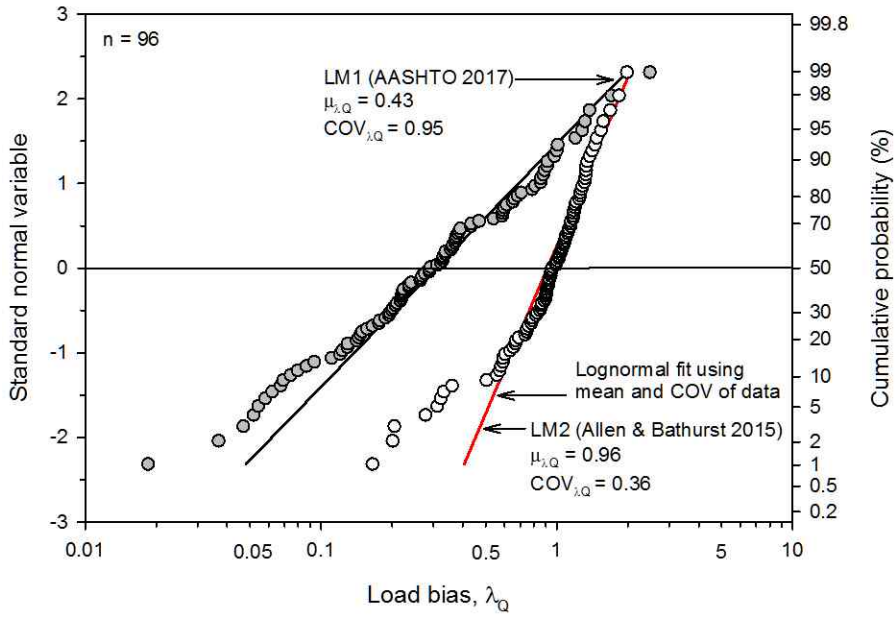

Figure 4. Cumulative distribution function (CDF) plots for load bias using two different load models

with the magnitude of the predicted pullout capacity. This is an undesirable outcome in principle for both allowable stress design and probabilistic design approaches. A preferred behaviour is that model accuracy does not change with predicted pullout capacity which is the case for pullout model (PM2) in this paper.

The strength of a linear correlation between X and Y in a plot of data such as Figure 5 can be quantified by Pearson's correlation coefficient (ρ) which is simply the R in R^2 used in linear regression analyses. Positive values are computed when Y increases with X, and negative values when Y decreases with X which is the case for pullout model (PM1) in Figure 5. Parameter ρ is an input parameter in Monte Carlo simulations using Equation 2.

Similar correlations can occur between nominal load ($Q_n = T_{max}$) and nominal resistance ($R_n = P_{max}$); such a case is illustrated in Figure 6 for the combination of poor load model (LM1) and poor pullout model (PM1) discussed previously. In this example, the correlation is because friction angle (ϕ) and unit weight (γ) appear in equations for T_{max} and P_{max} , and both soil parameters are sampled from the same populations during Monte Carlo simulation (i.e. the same friction angle and unit weight of soil contribute to tensile load and resistance in the pullout limit state equation).

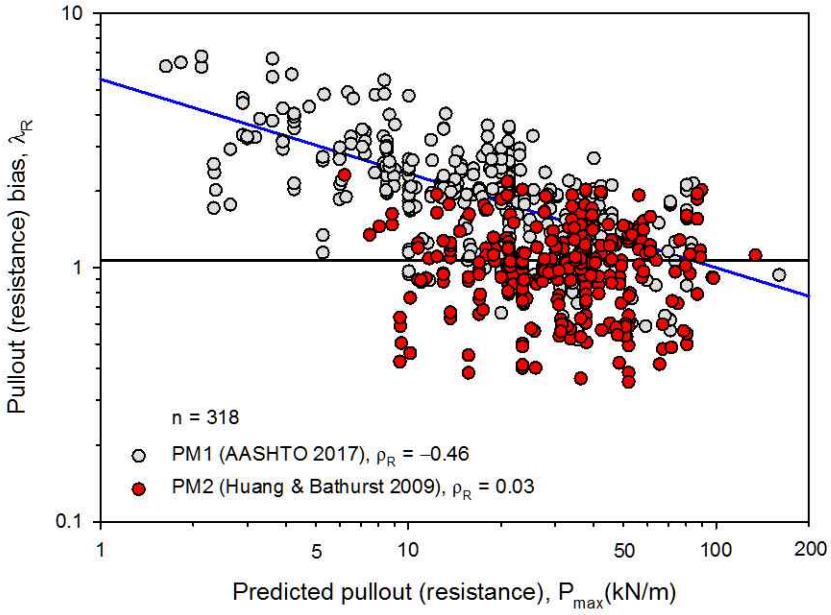

Figure 5. Example of pullout models with and without correlation between bias and predicted pullout capacity

4 CALCULATION OF PROBABILITY OF FAILURE (OR RELIABILITY INDEX)

The previous sections have described the formulation of a general limit state equation suitable for Monte Carlo simulation (Equation 2) and the random variables that appear in these analyses. However, engineers may not be comfortable with Monte Carlo techniques and the tools necessary to carry out these simulations. Fortunately, for the conditions described here and the observation that random variables for bias and nominal values are lognormally distributed, the following closed-form solution is available for the calculation of reliability index β introduced earlier (Bathurst and Javankhoshdel 2017):

$$\beta = \frac{\ln\left[\left(\frac{\mu_{\lambda R}}{\mu_{\lambda Q}}F_n\right)\sqrt{\frac{(1+COV_{Qn}^2)(1+COV_{\lambda Q}^2)}{(1+COV_{Rn}^2)(1+COV_{\lambda R}^2)}}\right]}{\sqrt{\ln\left[\frac{(1+COV_{Qn}^2)(1+COV_{\lambda Q}^2)(1+COV_{Rn}^2)(1+COV_{\lambda R}^2)(1+\rho_R COV_{Rn} COV_{\lambda R})^2(1+\rho_Q COV_{Qn} COV_{\lambda Q})^2}{(1+\rho_n COV_{Rn} COV_{Qn})^2}\right]}} \quad (5)$$

Here, $F_n = \mu_{Rn}/\mu_{Qn}$ is the nominal factor of safety which is the ratio of the mean of nominal resistance (R_n) and mean of nominal load (Q_n). This ratio is assumed equal to the ratio of nominal resistance (R_n) and nominal load (Q_n) used at time of design. This is the quantitative connection to factor of safety used in ASD. Quantities $\mu_{\lambda R}$ and $\mu_{\lambda Q}$ are mean values of nominal resistance and load *method bias* values (λ_R and λ_Q), respectively, and have uncertainty quantified by $COV_{\lambda R}$ and $COV_{\lambda Q}$ as discussed earlier. The nominal resistance (R_n) value and nominal load value (Q_n) used at design time in the limit state design equations also have uncertainty quantified by coefficients of variation denoted as COV_{Rn} and COV_{Qn}.

For reliability-based design the magnitudes of these COV values can be linked to the notion of *level of understanding* found in the Canadian Highway Bridge Design Code for LRFD of foundations (Fenton et al. 2016). Three levels of understanding are identified as high, typical and low; they are used to select matching resistance factors that increase in the order of low to high level of understanding. The choice of level of understanding captures the confidence of the designer with the choice of the model used to compute the nominal values for the project conditions, the amount and quality of the project data including material properties and knowledge of ground conditions, familiarity with the wall technology proposed and the applicability of the selected wall technology for the project works. Bathurst and Javankhoshdel (2017) mapped values of COV = 0.10, 0.20 and 0.30 to high, typical and low levels of understanding, respectively. Bathurst et al. (2017) gave an example how the engineer can self-evaluate to select the level of understanding that is appropriate for the case of the pullout limit state in a MSE wall project.

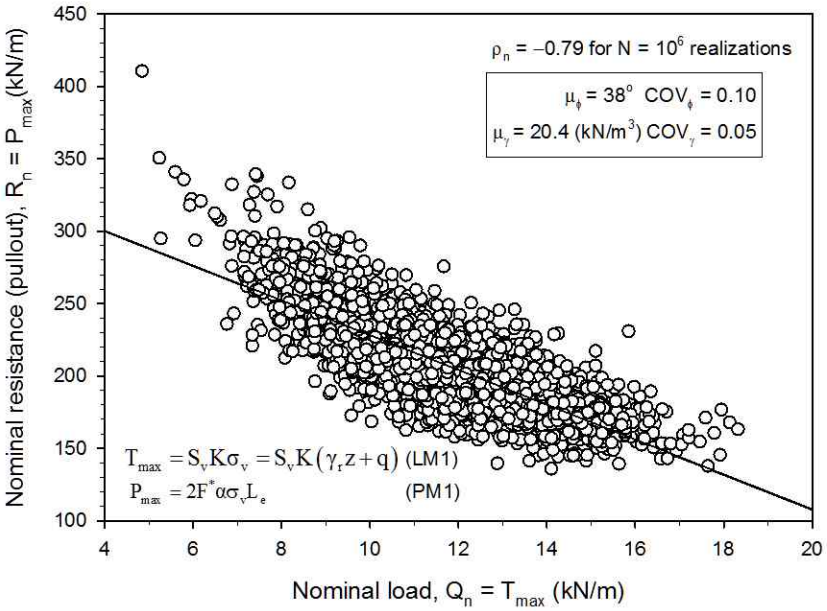

Figure 6. Example of negative correlation between nominal resistance (pullout) and nominal load (maximum tensile load) using combination of pullout model PM1 and load model LM1

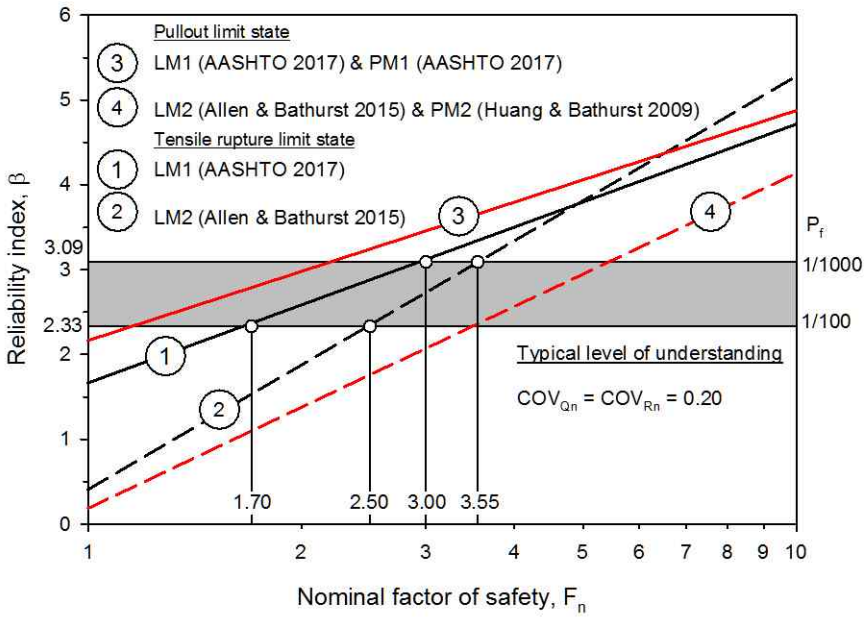

Figure 7. Reliability index β versus nominal factor of safety for tensile rupture and pullout limit states using different load and resistance models and typical level of understanding

Parameters ρ_R and ρ_Q are Pearson's correlation coefficients between variables R_n and λ_R, and between Q_n and λ_Q, respectively, and represent bias dependencies with nominal values described earlier. Parameter ρ_n is the correlation coefficient between R_n and Q_n and is called nominal correlation following the terminology introduced by Lin and Bathurst (2018). For the pullout limit state the soil material properties and their statistical characteristics are the same for the load equation associated with the active wedge in Figure 1 and the pullout equation associated with the resistant zone. Hence, $\rho_n \neq 0$ and will vary with changes in the distributions for friction angle and unit weight assumed at the location of each reinforcement layer as demonstrated by Lin and Bathurst (2018).

The mathematical relationship between probability of failure P_f and β has been given earlier in the paper. However, the advantage of Equation 5 is that it is easily implemented in a spreadsheet and generates smooth distributions of β when plotted against independent parameters of interest for sensitivity analyses during design.

Example calculation results are shown in Figure 7. For these calculations the level of understanding was taken as typical and the nominal correlation coefficient was taken as $\rho_n = -0.79$ from Figure 6 for the pullout limit state, and $\rho_n = 0$ for the tensile strength limit state (i.e. the load equation for T_{max} and

Equation 3 for T_{al} do not have common random variables). For the tensile rupture limit state the resistance side is the same for both cases identified in the figure (using Equation 3). However, the two load models for T_{max} (LM1 and LM2) described earlier are used in the tensile rupture limit state and in combination with the two pullout models (PM1 and PM2). Regardless of the choice of combination of load and resistance models for each limit state, as nominal factor of safety (F_n) increases so does the reliability index (or equivalently the probability of failure decreases), as expected. However, different load and resistance model combinations will give different margins of safety expressed as reliability index (or probability of failure) for the same nominal factor of safety and all other conditions remain the same.

Shown in Figure 7 are values of $\beta = 2.33$ and 3.09 that correspond to probabilities of failure of 1/100 and 1/1000, respectively. The smaller β value is recommended as the target minimum reliability index for internal limits states design and LRFD calibration for MSE walls. This value may appear small but MSE walls are highly strength-redundant systems. In other words, if one reinforcement layer fails, other layers can compensate and thus system failure is unlikely (Allen et al. 2005; Bathurst et al. 2008). Figure 7 shows that if a reinforcement layer is designed to just satisfy a target reliability of $\beta = 2.33$, the corresponding factor of safety using the poorer load model (LM1) is 1.70 while the same design with the more accurate load model (LM2) is higher at 2.50.

5 CONCLUSIONS

This paper is an attempt to describe a rational reliability theory-based approach for analysis and design of internal limit states for geosynthetic reinforced MSE walls. Nevertheless, the same concepts apply to other MSE wall types including soil nails and steel reinforced MSE wall systems. The application of the concepts described in this paper are particularly well-suited to MSE wall internal limit states analysis and design because the wall backfill soil and soil reinforcement materials are engineered materials, and the soil-structure limit states can be expressed by simple linear equations with known accuracy. This is not the case for other soil-structure problems in geotechnical foundation engineering (e.g. piles) where the soils are natural deposits and thus their properties are much more variable.

REFERENCES

Allen, T. M. and Bathurst, R. J. 2015. An improved simplified method for prediction of loads in reinforced soil walls. ASCE Journal of Geotechnical and Geoenvironmental Engineering 141(11): 04015049.

Allen, T. M. and Bathurst, R. J. 2018. Application of the Simplified Stiffness Method to design of reinforced soil walls. ASCE Journal of Geotechnical and Geoenvironmental Engineering 144(5): 04018024.

Allen, T. M., Nowak, A. S. and Bathurst, R. J. 2005. Calibration to Determine Load and Resistance Factors for Geotechnical and Structural Design. Transportation Research Board Circular E-C079, Washington, DC, 93 p.

AASHTO. 2017. LRFD Bridge Design Specifications, 8th Ed., American Association of State Highway and Transportation Officials (AASHTO), Washington DC. 73.

Bathurst, R. J., Allen, T. M. and Nowak, A. S. 2008. Calibration concepts for load and resistance factor design (LRFD) of reinforced soil walls. Canadian Geotechnical Journal 45(10): 1377-1392.

Bathurst, R. J., Huang, B. and Allen, T. M. 2011. Analysis of installation damage tests for LRFD calibration of reinforced soil structures. Geotextiles and Geomembranes 29(3): 323-334.

Bathurst, R. J. and Javankhoshdel, S. 2017. Influence of model type, bias and input parameter variability on reliability analysis for simple limit states in soil-structure interaction problems. Georisk 11(1): 42-54.

Bathurst, R.J., Javankhoshdel, S. and Allen, T.M. 2017. LRFD calibration of simple soil-structure limit states considering method bias and design parameter variability. ASCE Journal of Geotechnical and Geoenvironmental Engineering 143(9): 04017053-1-14.

Bathurst, R. J. and Miyata, Y. 2015. Reliability-based analysis of combined installation damage and creep for the tensile rupture limit state of geogrid reinforcement in Japan. Soils and Foundations 55(2): 437-446.

Fenton, G. A., Naghibi, F., Dundas, D., Bathurst, R. J. and Griffiths, D. V. 2016. Reliability-based geotechnical design in the 2014 Canadian Highway Bridge Design Code. Canadian Geotechnical Journal 53(5): 236-251.

Huang, B. and Bathurst, R. J. 2009. Evaluation of soil-geogrid pullout models using a statistical approach. ASTM Geotechnical Testing Journal 32(6): 489-504.

Lin, P. and Bathurst, R.J. 2018. Influence of cross-correlation between nominal load and resistance on reliability-based design for simple linear soil-structure limit states. Canadian Geotechnical Journal 55(2): 279-295.

Miyata, Y. and Bathurst, R. J. 2012. Analysis and calibration of default steel strip pullout models used in Japan. Soils and Foundations 52(3): 481-497.